

Total Body Surface Potential Mapping During Exercise: QRS-T-wave Changes in Normal Young Adults

WALTER T. MILLER III, PH.D., MADISON S. SPACH, M.D., AND ROBERT B. WARREN, PH.D.

SUMMARY Total body surface potential distributions were recorded from 20 normal young adults, 20–35 years old, during multistage maximal exercise testing on a bicycle ergometer. Using a system for measuring total body surface potential distributions from measurements at 24 locations, high-quality potential maps were obtained during exercise without requiring wave form averaging or special modes of exercise. Serial maps recorded at 1-msec intervals throughout QRS-T during exercise and during recovery from exercise were compared with corresponding maps recorded with the subjects at rest. During and after exercise, consistent changes appeared in the map patterns during early QRS and the ST segment and in the magnitude of the T-wave potentials. Increases in QRS duration (0–10 msec) also appeared during exercise. The changes in map patterns during early QRS in exercise strongly suggested changes in the initial sequence of activation in the ventricles. The results demonstrate the importance of analyses of total body surface potential distributions in understanding ECG changes during exercise.

CHANGES in electrocardiographic wave form shape in response to exercise in both normal subjects and cardiac patients have been described extensively. Most descriptions pertain to exercise-induced changes in ventricular repolarization as expressed in the ST segment and T wave of the body surface ECG.¹ Depression of the J point (upsloping ST-segment depression) in left precordial leads is considered a normal response to exercise. The development of horizontal or downsloping ST-segment depression in precordial leads during or immediately after exercise is suggestive of regional myocardial ischemia. The statistical relationship of ST-segment depression during exercise to narrowing of the coronary arteries as revealed by coronary angiographic studies has been extensively investigated, as reviewed by Fortuin and Weiss.¹

R-wave magnitude changes in left precordial leads during exercise in both normal and abnormal subjects have also been described.^{2–5} In general, a decrease in R-wave magnitude is considered a normal response to exercise, while an increase in R-wave magnitude is considered abnormal. Bonoris and co-workers have suggested that inclusion of such R-wave magnitude changes in diagnostic criteria along with ST-segment changes would enhance the ability of the stress ECG to detect coronary artery disease.^{6–8}

An important limitation in the use of electrocardiographic criteria to distinguish between normal and abnormal responses to exercise results from an incomplete understanding of the physiologic mechanisms underlying the observed changes in wave form

shape. The most common measurement of the ECG during exercise is from a single bipolar lead with the positive electrode on the left chest at the position of the standard lead V₆, and the negative electrode on the right chest, head or back.¹ When such measurements from a single lead are used, it is often difficult to distinguish changes in the ECG corresponding to exercise-induced alterations in the sources of current within the myocardium from changes in the ECG related to changes in heart position or volume conductor geometry. This is especially true when trying to interpret the relatively subtle changes often observed in ECG wave forms recorded during exercise in normal subjects (J-point depression and R-wave magnitude changes). When major changes in wave form shape occur during exercise, such as deep ST-segment depression or T-wave inversion, abnormal changes in the cardiac electrical sources are clearly indicated. Measurements from a single lead, however, provide little information about the nature and spatial distribution of the electrophysiologic changes in the heart. As a result, “normal” and “abnormal” ECG responses to exercise are usually defined on the basis of statistical correlations between coronary angiographic studies and various parameters derived from the ECG wave form, such as ST-segment depression 60 or 80 msec after the J point¹ or change in R-wave magnitude,^{6–8} rather than in terms of electrical events in the heart.

Several investigators have proposed the use of multiple-lead systems to increase the diagnostic usefulness of the exercise ECG. These lead systems include the standard 12 leads,^{9–11} orthogonal vector leads,^{12–16} left precordial surface maps,^{17–19} and total body surface isopotential maps.^{20, 21} Although such multiple-lead systems may reveal more information about the electrophysiologic state of the heart, they are still difficult to use for interpreting recorded ECG wave forms directly in terms of the underlying cardiac electrical events. Left precordial surface maps present spatial (as well as temporal) information about the ECG, but only for a limited region on the torso. Total

From the Departments of Biomedical Engineering, Pediatrics, and Physiology, Duke University Medical Center, Durham, North Carolina.

Supported in part by USPHS grants HL11307, HL05716 and HL07101.

Address for correspondence: Walter T. Miller III, Ph.D., Department of Electrical and Computer Engineering, Kingsbury Hall, University of New Hampshire, Durham, New Hampshire 03824.

Received November 2, 1979; revision accepted February 11, 1980.

Circulation 62, No. 3, 1980.

body surface isopotential maps are the most useful for making such interpretations of the ECG because spatial distributions of potentials over the entire torso at sequential instants of time in each cardiac cycle can be examined.

Body surface mapping lead systems sometimes use as many as 100 to 200 electrodes. The practical problems involved in recording low noise signals simultaneously from such large electrode arrays during moderate or maximal exercise have resulted in only limited application of isopotential surface mapping to the study of the exercise ECG. However, techniques for accurately estimating total body surface potential distributions from measurements at 20–30 select locations on the torso also have been reported.^{22–26} Using one such limited lead system,²⁶ we developed a practical system for recording and processing total body surface isopotential maps during exercise.²⁷ In this study we examined body surface potential distributions throughout ventricular activation and repolarization in normal young adult subjects at rest, during multistage maximal exercise procedures and during recovery from exercise.

Methods

Selection of Subjects

For this study, normal young adult volunteers, ages 20–35 years, were recruited from the staff at Duke University and Duke Hospital. Ten male and 10 female subjects were selected. All subjects had normal resting ECGs as judged from both the standard 12 leads and body surface isopotential maps, and none had a history of cardiovascular disease. All subjects were considered to be in good general physical condition. None were trained endurance athletes. Cardiac catheterization data were not available for any sub-

ject. In all subjects, the resting blood pressure was normal (less than 140/90 mm Hg).

Lead System

The lead system used was based on the limited lead system for isopotential body surface mapping derived by Warren et al.^{25, 26} This system allows the accurate estimation of potentials at 150 locations on the body surface (covering the chest, sides and back) with respect to Wilson's central terminal, starting from potential measurements at a subset of 24 of the 150 locations (fig. 1). Recording potentials from limb lead electrodes during exercise presented obvious problems of motion artifact. Therefore, potentials in this study were measured with respect to a single reference electrode on the back (fig. 1) rather than with respect to Wilson's central terminal, and a variation of the transformation matrix for estimating the 150 map potentials was derived for use with potentials referenced to the single-back electrode. At the same time, transfer coefficients for estimating the potential of Wilson's central terminal from the 24 potentials measured with respect to the back reference location were also derived. Combining these results provided a single transformation matrix that estimated the potentials at the 150 mapping locations with respect to Wilson's central terminal, starting from the 24 potentials measured with respect to the single back electrode. This transformation matrix was used for all maps presented in this study during rest or exercise.

The potentials at the 24 locations on the body surface were measured using two commercially produced 15-lead shielded ECG cable systems (NDM 04-2000) and disposable silver/silver chloride ECG stress test electrodes (AMI 1555-005). The ECG cables were connected to the inputs of 24 AC-coupled amplifiers that had flat frequency responses of 0.1–30,000 Hz.

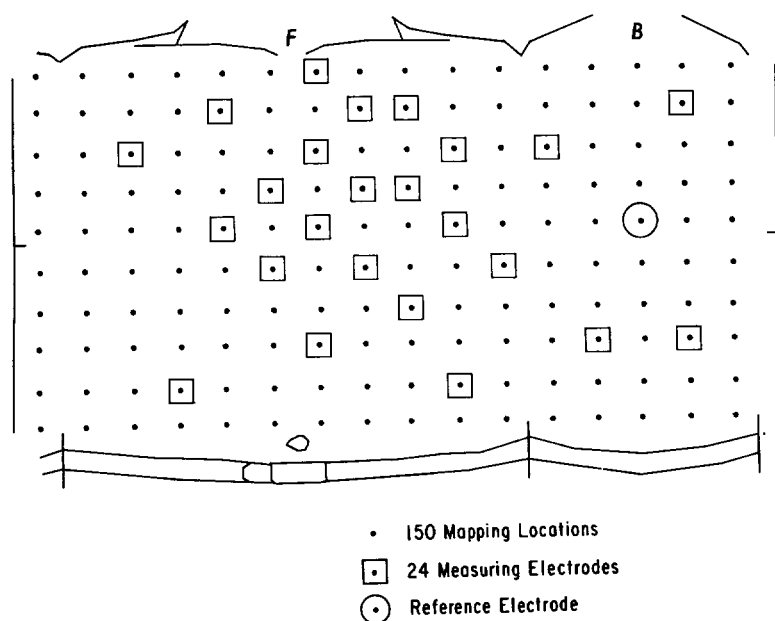


FIGURE 1. Body surface mapping lead system. The approximate locations of the 150 points at which the body surface potentials were calculated are indicated by dots on the torso drawing. For continuity, the columns shown at the extreme left and right in the figure represent the same mapping locations on the right back. The locations of the 24 measuring electrodes are indicated by squares. The location of the single reference electrode is indicated by a circle. The mapping location used to approximate the standard lead V_6 was in the sixth row from the top and in the seventh column from the right of the figure.

The analog signals were then digitized for display and storage using a PDP-11/20 data acquisition system that was described in detail by Barr et al.²⁸ The analog signals were sampled at a rate of 1000 samples/sec per channel (12-bit samples) for 1560 msec (one "block" of data).

Exercise Protocol

Multistage maximal stress test procedures were performed in an upright position on a Cybex Fitron bicycle ergometer. Each subject started exercise at a work rate of 300 kilopond meters/min* (kpm/min). Thereafter, the work rate was increased by 300 kpm/min every 4 minutes. The pedaling rate was held constant at 60 rpm. Exercise was stopped upon complaint of fatigue by the subject, regardless of the maximal heart rate achieved.

Before beginning the exercise procedure, three to five blocks of data were recorded with the subject at rest, sitting on the bicycle. During exercise, ECG wave forms were sequentially sampled, displayed on a Tektronix 4014 display unit, and either stored on digital magnetic tape or discarded, depending on the investigator's evaluation of the level of artifact. Blocks of data were recorded for approximately 10 minutes after cessation of exercise while the subject rested while still seated on the bicycle. Emphasis was placed on obtaining low-noise data at all stages of exercise. Therefore, recordings were obtained 25–35 times from each subject, including data recorded during rest, exercise and recovery.

The value of the computer's time-of-day clock (in units of hours, minutes and seconds) at the beginning of each sampling interval was automatically stored with each set of ECG wave forms on digital tape. The investigator manually recorded the clock value at the beginning of exercise, each time the work rate was increased, and when exercise was stopped. During later data analysis, these clock values provided a precise documentation of when, during the exercise protocol of the subject, each particular sequence of maps had been recorded.

Data Processing and Baseline Adjustment

The digitized wave forms in the block of data to be processed were first read from the magnetic tape and displayed. Generally, some degree of baseline drift was visible in the wave forms (fig. 2A). The computer operator used the cursors of the display unit to identify the same instant of time (referred to as the voltage reference time) in each cardiac cycle of one ECG wave form. The selected time instants were defined to be times in the cardiac cycle at which the potentials of all of the ECG wave forms would be designated as zero voltage. Thus, the voltages of the wave forms at the selected time instants represented estimates of the voltages of the baseline offsets. For low heart rates,

voltage reference times have usually been chosen during the UP interval.²⁹ At high heart rates, however, the U and P waves merge and this combined wave intersects with the latter portion of the T wave, such that an isoelectric UP or TP interval no longer exists. In such instances the best choice for a baseline reference is the end of the PR segment.^{3, 29–31} For consistency in this study, both resting and exercise maps were processed, using voltage reference times chosen near the end of the PR segment. Figure 2B shows the wave forms of panel A with four voltage reference times chosen just before the QRS complexes. Although only six wave forms are shown in the figure, the same voltage reference times were used for all 24 ECG wave forms in a given block of data.

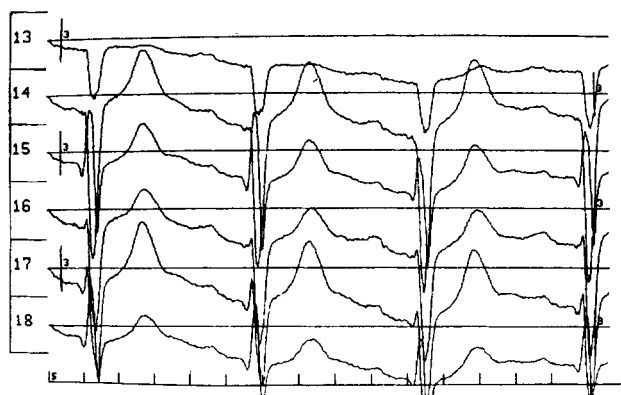
A linear interpolation technique for baseline adjustment²⁹ was used when all wave forms had constant baseline offset or linear baseline drift. When nonlinear baseline drift was present in one or more wave forms (fig. 2A), a nonlinear baseline compensation technique reported by Meyer and Keiser³² was used to estimate the baseline offsets of the 24 wave forms at each instant of time (corresponding to each data sample) from the potentials at the voltage reference times. The computed baseline offsets were then subtracted from the measured wave forms, resulting in 24 "baseline-compensated" wave forms. Figure 2C shows the wave forms from panel A after baseline compensation and figure 2D shows the corresponding computed baseline offsets. The nonlinear adjustment worked well for most baseline drifts. When rapid or abrupt changes in baseline offset occurred in the wave forms, however, the technique was not adequate and the data block was not used. The number of baseline voltage reference times in each block of data increased with increasing heart rate, so the technique for nonlinear baseline adjustment was best suited to high heart rates.

After baseline adjustment, a computer program automatically computed the potentials at the 150 locations at each instant of time, displayed them in surface map format, drew the isopotential contour lines, and photographed the map on 16-mm film. The potential wave form at the mapping location nearest to the location of the standard precordial lead V_6 was displayed below each map as a time reference wave form. For simplicity, this potential wave form will be referred to throughout the paper as lead V_6 . Maps were displayed for each millisecond during QRS and every fourth millisecond during other intervals. Photographing the maps sequentially on 16-mm film allowed subsequent instant-by-instant and motion analysis of the maps.

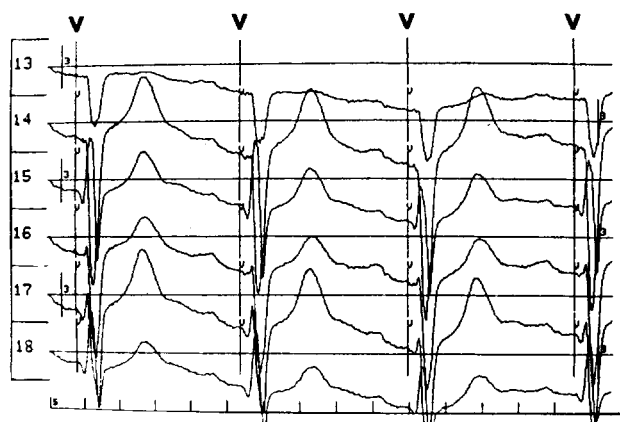
The root mean square (RMS) map potential wave forms presented in the results were obtained as follows: For each instant of time in a given block of data, the RMS value of the estimated potentials at the 150 mapping locations was calculated. The resulting RMS potentials at 1-msec intervals (for the total block time of 1560 msec) were automatically displayed as a potential wave form and photographed on 16-mm film.

*Kilopond meter: work done in lifting a 1-kg mass 1 M, assuming the standard gravitational acceleration.

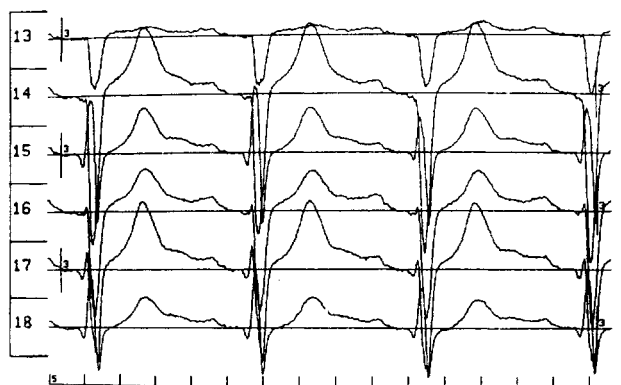
A. MEASURED WAVEFORMS



B. BASELINE ID.



C. AFTER BASELINE COMPENSATION



D. COMPUTED BASELINES

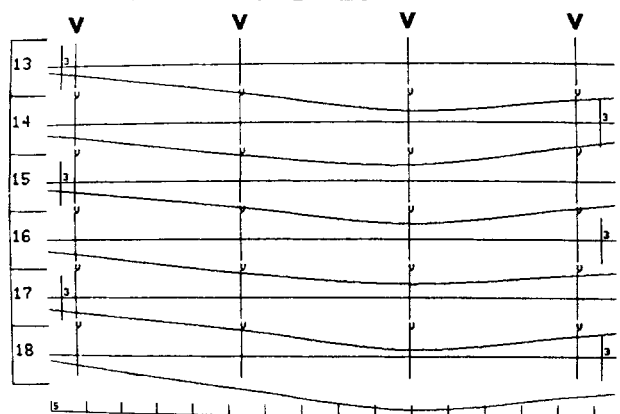


FIGURE 2. Nonlinear baseline compensation. (A) Digitized ECG wave forms from six of the 24 channels. The vertical line to the left or right of each wave form indicates 1 mV of potential. Each division on the horizontal time scale below the six wave forms indicates 100 msec. (B) The four vertical lines through each wave form below the large "V" identify the times selected by the investigator as voltage reference times for baseline compensation. (C) The six ECG wave forms after subtraction of the computed baselines. (D) The computed baselines are displayed with the same voltage and time scales as the original measured wave forms in panel A. The voltage reference times used to compute the baselines are also shown.

Results

All subjects showed a normal electrocardiographic response to exercise in lead V_5 . ST-segment depression in this lead was limited to low-magnitude (less than 200 μ V) J-point depression. No horizontal or downsloping ST-segment depression or T-wave inversion was observed. The magnitude of the R wave in lead V_5 decreased during exercise for 16 subjects and stayed nearly the same for four subjects. No subject had arrhythmias during or after exercise, and no subject experienced chest pain. Maximal heart rates ranged from 170–195 beats/min.

The body surface isopotential maps at rest varied from subject to subject within the limits of normal variability.^{33, 34} Similarly, maps recorded during exercise varied from subject to subject. Consistent map changes were observed, however, when the exercise

and postexercise maps were compared with the resting map of the same subject. Accordingly, the resting and exercise maps we present were chosen as being representative of the changes observed, although there were individual variations in map patterns that will not be shown. No obvious group differences were observed between the exercise-induced changes in map patterns of male and female subjects.

QRS

Figures 3–6 show body surface isopotential maps recorded at rest and during exercise from a normal 25-year-old female subject. The resting map was recorded with the subject sitting upright on the bicycle ergometer, with a heart rate of 75 beats/min. The exercise maps were recorded 10 minutes and 52 seconds after the start of the multistage exercise procedure, at

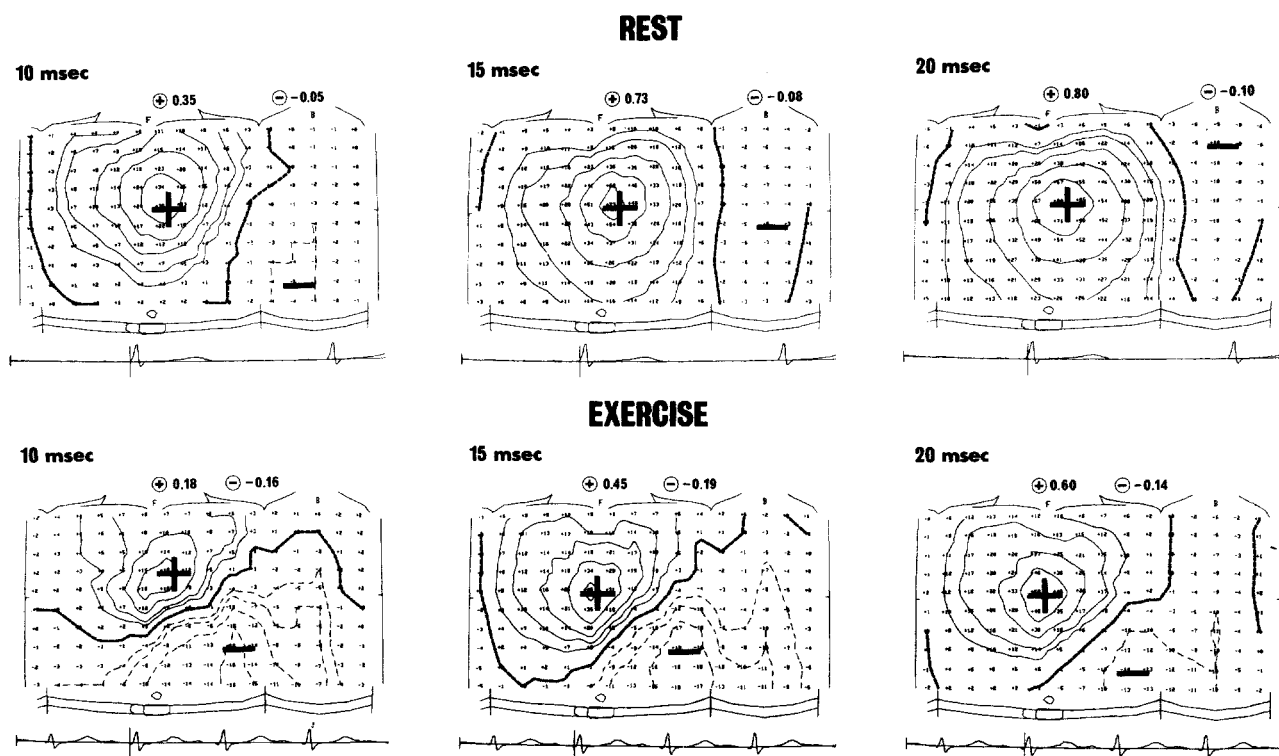


FIGURE 3. QRS maps at rest and during exercise. Body surface potential distributions at three instants of time during early QRS at rest and during exercise are shown. To the upper left of each map, the approximate time with respect to the beginning of ventricular activation is indicated in milliseconds. The format of each map panel is as follows: The map geometry is the same as that in figure 1. The potential at each of the 150 mapping locations is shown in $10\text{-}\mu\text{V}$ units. Generally, these numbers are too small to be seen clearly in the final published figures, but they serve to mark the mapping locations. Absolute and relative potential maxima and minima are indicated by large plus and minus symbols, respectively, adjacent to the corresponding map locations. The magnitudes of these features are indicated above the maps in millivolt units. Contour lines are drawn according to a logarithmic scale to represent the following values in microvolts: 40, 60, 100, 150, 250, 400, 600, 1000, 1500, 2500, 4000, 6000 and 10,000. Negative contours are drawn as dashed lines. Zero potential contours are drawn as heavy dashed lines. The estimated lead V_6 ECG is shown below each map frame as a time reference trace. A vertical line is drawn through the wave form at the time instant represented by the map. The vertical line at the extreme left of the time reference trace indicates 1 mV of potential. The total time in the time reference trace is 1560 msec.

a work rate of 900 kpm/min. The subject's heart rate was 168 beats/min.

At rest, the potential distributions during early QRS (fig. 3) were characterized by a dominant anterior potential maximum, with a minimum of lower magnitude on the lower left back. The minimum moved slowly up the back as QRS progressed, and the anterior maximum became greater in magnitude. During exercise, the potential distributions representing early QRS were quite different. The early potential minimum was on the lower left chest and was similar in magnitude to the potential maximum. As QRS progressed, the minimum at first increased in magnitude and then decreased, moving toward the lower left side and back, while the maximum increased in magnitude and covered more of the area of the anterior torso.

Approximately 25 msec into QRS (fig. 4), right ventricular breakthrough patterns appeared in both the resting and exercise maps. The resting map at 25 msec showed a "saddle" distribution, similar to that described by Taccardi,³⁸ the negative potential area

projecting down from the vicinity of the upper right sternum. The pattern of the exercise map at 25 msec was unusual. The anterior breakthrough minimum split the early anterior potential maximum into two separate potential maxima of lower magnitude, one on the upper right chest and one on the precordium.

The magnitude of the prominent anterior precordial minimum in both the resting and exercise maps grew rapidly. In the resting map at 30 msec, the magnitude of the central minimum was nearly equal to that of the potential maximum to the lower left. A second minimum of lower amplitude persisted on the upper right chest. The spatial locations of the potential maximum and minimum of largest magnitude in the exercise map at 30 msec were similar to those in the resting map. The magnitude of the lower left potential maximum, however, was only half of the magnitude of the corresponding maximum in the resting map (0.54 mV vs 1.12 mV). The central minimum was similar in magnitude to that of the resting map, but the area of negative potentials in the exercise map extended lower on the right chest. The

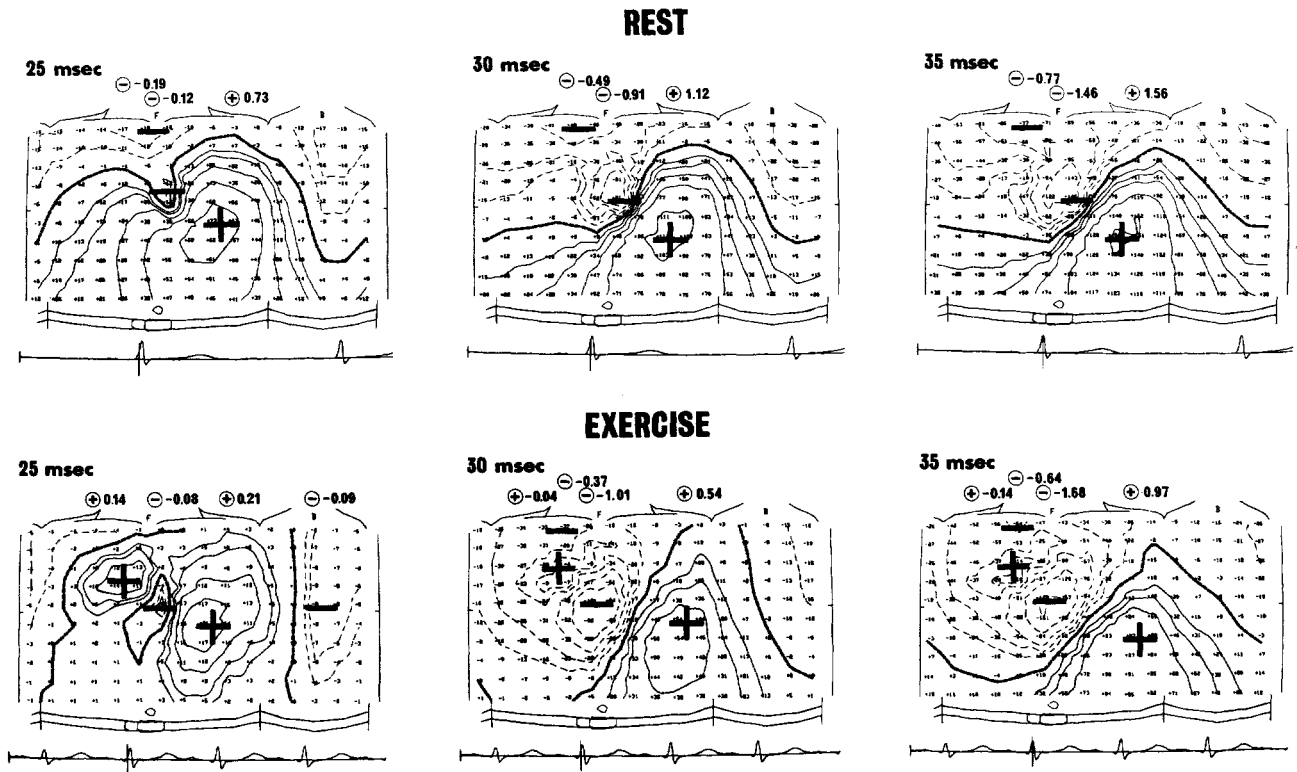


FIGURE 4. QRS maps at rest and during exercise. See text.

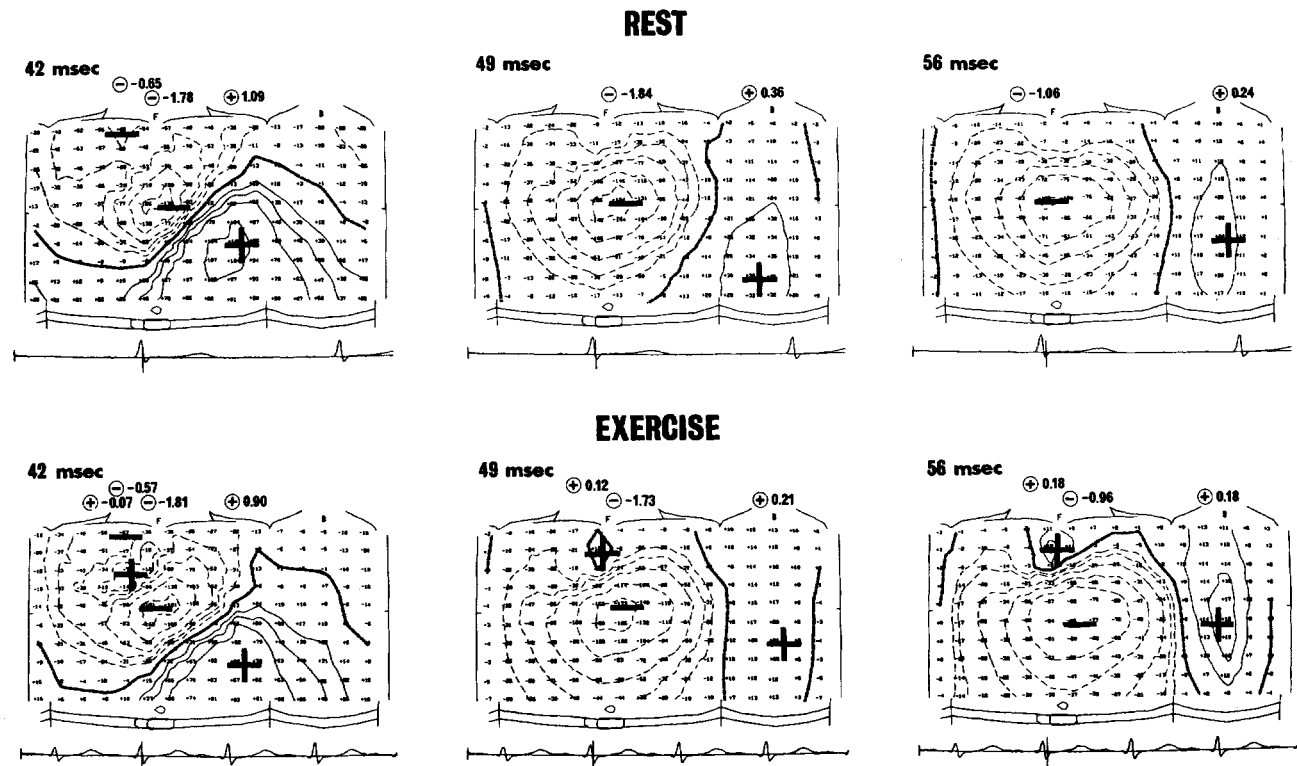


FIGURE 5. QRS maps at rest and during exercise. See text.

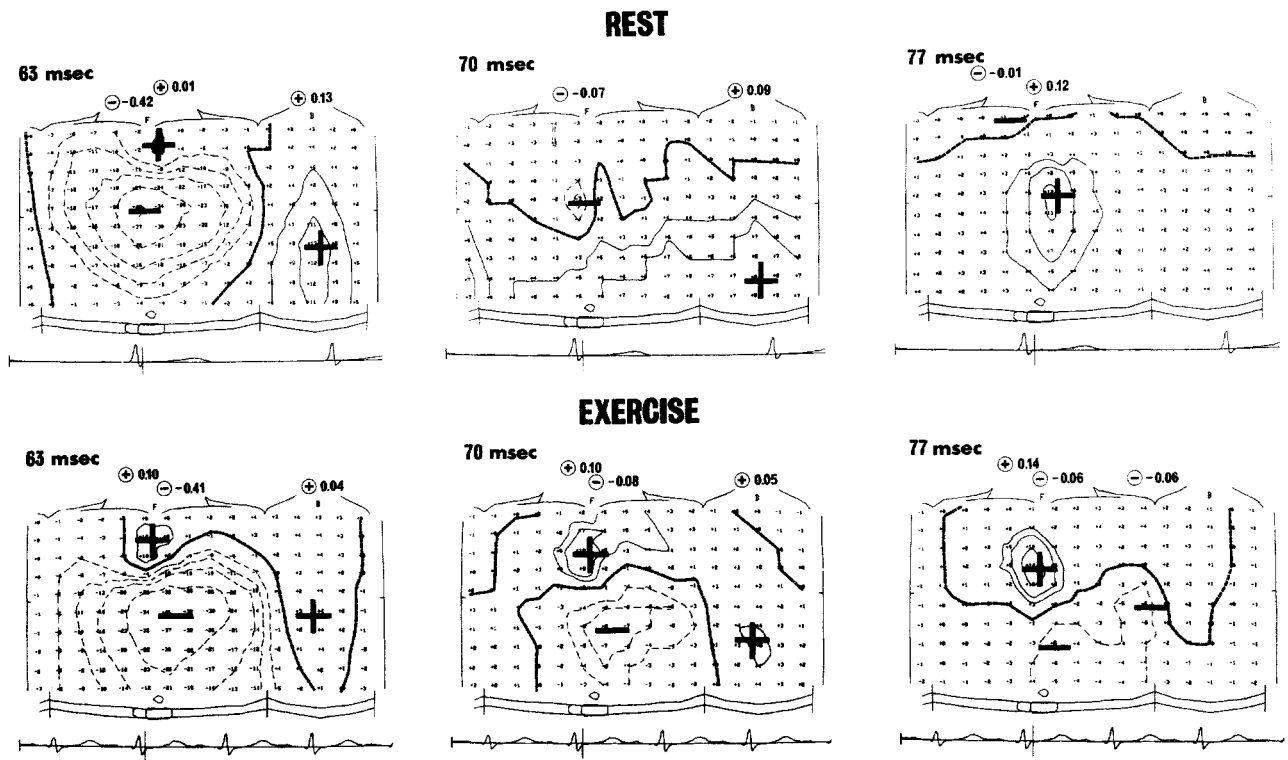


FIGURE 6. QRS maps at rest and during exercise. See text.

potential maximum on the upper right chest in the exercise map at 25 msec appeared in the map at 30 msec as a relative potential maximum in the negative potential region, completely surrounded by negative potentials of larger magnitude. It is interesting to compare this distinct potential maximum in the negative region of the exercise map, separating the two potential minima, with the curvature of the contour lines between the corresponding two potential minima in the resting map at 30 msec.

The general features of the resting and exercise maps at 30 msec persisted throughout the middle of QRS, as shown in the maps at 35 msec (fig. 4) and 42 msec (fig. 5). Although there was little spatial movement in the patterns during this period, there was considerable variation in the magnitudes of the maxima and minima. Near the peak of the R wave in lead V_5 (fig. 4), the magnitude of the lower left potential maximum in the exercise map was approximately 60% of that in the map at rest (0.97 mV compared with 1.56 mV). The central potential minimum at this time was slightly larger in magnitude in the exercise map (-1.68 mV) than in the map at rest (-1.46 mV). Between 35 msec and 42 msec the magnitude of the lower left potential maximum in the resting map decreased relatively faster (from 1.56 mV to 1.09 mV) than in the exercise map (from 0.97 mV to 0.90 mV), so that at 42 msec the magnitudes of this maximum at rest and during exercise were more nearly equal. The magnitudes of the central anterior minimum at 42 msec were also similar at rest (-1.78 mV) and during exercise (-1.81 mV).

By 49 msec into QRS (fig. 5), the potential max-

imum that was previously on the lower left chest had decreased greatly and had moved to the lower back in both the resting and exercise maps. The central potential minimum in both maps had changed little from the maps at 42 msec, but the negative potential region had grown to cover most of the anterior torso. In the exercise map at 49 msec the relative potential maximum that was in the negative region of the earlier maps during exercise had moved to the upper sternal region and had become positive in sign. The curvature of the negative potential contours in the upper sternal region of the map at rest was suggestive of the upper sternal maximum in the exercise map, but no distinct potential maximum was present in this region in the resting map.

After 49 msec, the magnitudes of the central anterior minimum in both the resting and exercise maps decreased rapidly with time (figs. 5 and 6), but at each instant the magnitudes of this minimum in the resting and exercise maps were nearly the same. The upper sternal maximum in the exercise maps reached a peak value near 56 msec (0.18 mV) and then decreased. At 63 msec a distinct upper sternal maximum with a small absolute magnitude (0.01 mV) was also present in the resting map.

The potentials in both the resting and exercise maps at 70 msec (fig. 6) were low in magnitude, but the major features of terminal QRS could still be seen. Note the positive potentials projecting upward into the negative region next to the central anterior minimum of the resting map. Serial inspection of the maps at each millisecond indicated that this was the early appearance of the repolarization maximum shown in

the map at 77 msec. Similarly, serial comparison of the maps during exercise showed that at 70 msec the upper anterior maximum was between the location of the terminal QRS sternal maximum and the location of the early recovery maximum at 77 msec. Thus, the patterns at rest and during exercise at 70 msec showed the effects of both terminal activation and early repolarization.

The resting map at 77 msec showed a pattern typical of potential distributions of normal subjects during the early ST segment.^{34, 36} The pattern was dominated by an anterior maximum with a distributed region of low level negative potentials near the right shoulder. Similarly, during exercise the feature with the largest magnitude at 77 msec was the anterior potential maximum. The region of negative potentials, however, was larger in magnitude than in the resting map and was located on the lower left of the potential maximum.

To further investigate the changes in body surface potentials during exercise, the RMS map potential was calculated at each instant of time during QRS and displayed as an RMS potential wave form. Figure 7A shows the RMS map potential wave forms at rest and during exercise corresponding to the body surface maps from the female subject shown in figures 3-6.

For comparison with other subjects, panels B, C and D show the RMS map potentials during QRS from a 23-year-old male, a 35-year-old male, and a 28-year-old male. The resting and exercise RMS wave forms in each panel are time-aligned at the beginning of QRS.

The most striking change in the RMS map potential wave forms during exercise was the development of an initial low-level peak immediately preceding the major rise in RMS potential, with an associated increase in the time between the beginning of QRS and the major potential rise (2-10 msec).

Comparison of the RMS potential wave forms with the map patterns showed that the period preceding the initial peak in the RMS wave forms during exercise corresponded to the times when the early minimum was present on the lower left chest (fig. 3, exercise), while the drop in potentials after the peak corresponded to the approximate time of right ventricular breakthrough (fig. 4). Due to the delay in the major rise of the RMS potentials, the drop in potentials after the initial peak of the RMS wave form was generally more distinct during exercise, and as a result, the RMS potential magnitudes near the time of breakthrough were lower than in the corresponding maps at rest. The rapid rise in the RMS potential

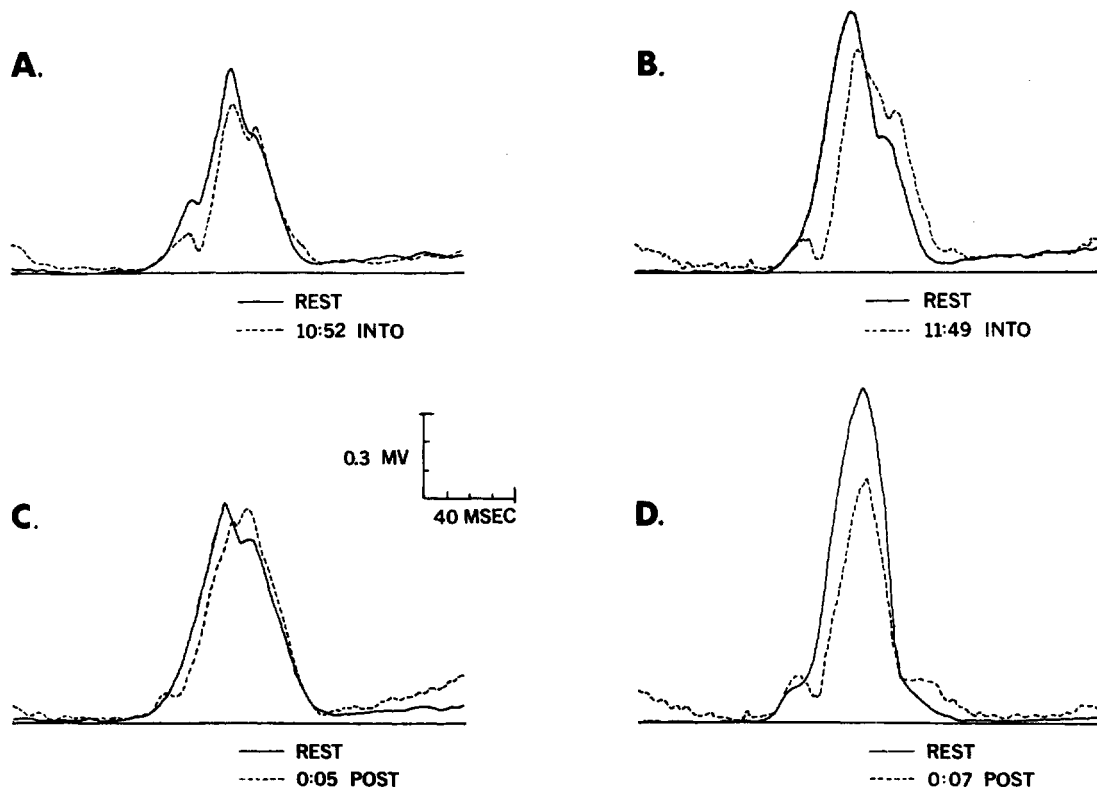


FIGURE 7. Root mean square (RMS) map potential wave forms. RMS potential wave forms during QRS are shown for four subjects at rest and either during exercise (A and B) or immediately after exercise (C and D). In each panel, the solid line represents the RMS potential wave form at rest and the broken line represents the wave form during or after exercise. The horizontal time scale in the center of the figure is divided into 10-msec segments for 40 msec. The vertical voltage scale is divided into 0.1-mV segments for 0.3 mV.

wave form before the major peak corresponded to the rapid increase in magnitude of the central anterior minimum and lower left maximum after breakthrough (fig. 4).

The magnitude of the major peak of the RMS potential wave form tended to be less during exercise than at rest (fig. 7). In the resting and exercise maps of all subjects, the pattern of potentials near the time of the major peak of the RMS wave form was dominated by a central anterior potential minimum and an anterior maximum on the lower left torso (figs. 4 and 5). The peak magnitude of the potential maximum in the exercise maps was consistently less than the peak magnitude of the maximum in the corresponding maps at rest. The changes in magnitude of the large central potential minimum were less consistent, however, although increases in magnitude were sometimes observed during or after exercise. During exercise there was also an increase in the magnitude of a third peak, or the development of a third peak, in the RMS potential wave form. This peak corresponded in time to the appearance of the upper sternal maximum (fig. 5) in the surface potential distribution.

The changes in shape of the RMS wave forms during exercise were sometimes accompanied by apparent changes in QRS duration (figs. 7B and D). Noise during exercise in the low-level map patterns at the beginning of QRS and early repolarization potentials at the end of QRS caused some uncertainty in the measurements of QRS duration during exercise. As a result, small changes in QRS duration could not be detected with confidence. For some subjects, however, an increase in QRS duration was clearly evident. Both the serial body surface potential distributions and the RMS potential wave forms revealed an apparent increase in QRS duration during exercise for 11 of the 20 subjects, with a maximum increase of 8–10 msec.

The changes observed in the body surface potential distributions during QRS have been described in terms of resting maps and exercise maps. Actually, data were recorded periodically throughout the exercise procedure and for 10 minutes after exercise. Thus, for each subject there was a series of maps showing gradual changes during and after exercise. In general, the greatest changes in the maps during QRS were seen when comparing the maps recorded at rest with those recorded near the peak of exercise or in the first seconds after exercise. The map patterns at earlier stages of exercise tended to fall somewhere between the resting map patterns and those at the peak of exercise, and similarly those recorded after exercise appeared to gradually change back to the patterns recorded at rest. However, the intermediate changes in QRS map patterns during exercise and those after exercise were not exactly the same. For example, some subjects immediately after exercise had an increase in the magnitude of the RMS potentials in mid-QRS (contrasted to the decrease in peak RMS potentials during exercise), associated mainly with an increase in the magnitude of the central anterior minimum (up to 1 mV of change) without a change in the overall pattern of the potentials. Also, the intermediate

pattern changes observed during and after exercise were not symmetrical with respect to heart rate, i.e., QRS-map changes persisted to lower heart rates after exercise than the heart rates at which the changes initially developed during exercise. Further analysis is required to more specifically differentiate intermediate QRS-map changes during and after exercise.

ST Segment

Figure 8 shows body surface potential distributions during the early ST segment from a 29-year-old male (panel A) and a 25-year-old male (panel B) at rest, during exercise, and during recovery from exercise. The maps at rest are typical of the potential distributions observed during the ST segment in normal adult subjects.^{34, 35} The map patterns are characterized by an anterior potential maximum on the left chest, with low-level negative potentials distributed over the right shoulder and back.

During exercise, all of the subjects studied had an increase in negativity on the lower anterior torso during the early ST segment.²⁰ Most often, a potential minimum developed on the lower left precordium (figs. 6 and 8). The region of negative potentials sometimes extended to the lower right chest as well (fig. 8B). The lower anterior negativity persisted after exercise but was generally smaller in magnitude than at high work rates during exercise. The negative ST-segment potentials shown in figure 8A during exercise were among the largest-magnitude negative potentials observed in the ST-segment maps. Although the negative ST-segment potentials in the exercise maps were generally larger than those in the corresponding maps at rest, no consistent differences were found between the magnitudes of the RMS-map potentials of the early ST segment at rest and during exercise (fig. 7). The negative potentials in the lower left precordial region during the early ST segment decreased steadily and were usually positive by the early portion of the T wave.

T Wave

Figure 9 shows typical body surface potential distributions at the peak of the T wave from a 35-year-old male subject at rest, during exercise, at the end of exercise and during recovery from exercise. Little change occurred in the basic pattern of the T-wave maps during and after exercise. The patterns of the peak T-wave maps were characterized by a large potential maximum on the left chest. Changes in the position of the potential minimum during exercise were noted, but its position was confined to the region of the right clavicle, right shoulder and back.

Although the pattern of the potentials at the peak of the T wave stayed relatively constant during and after exercise, considerable variation in T-wave magnitude was noted, in agreement with previous studies of ECG wave forms from scalar precordial leads and orthogonal vector leads during exercise^{2, 15, 36-40} At the peak of exercise, the magnitude of the maximum map potential during the T wave increased more than 0.1

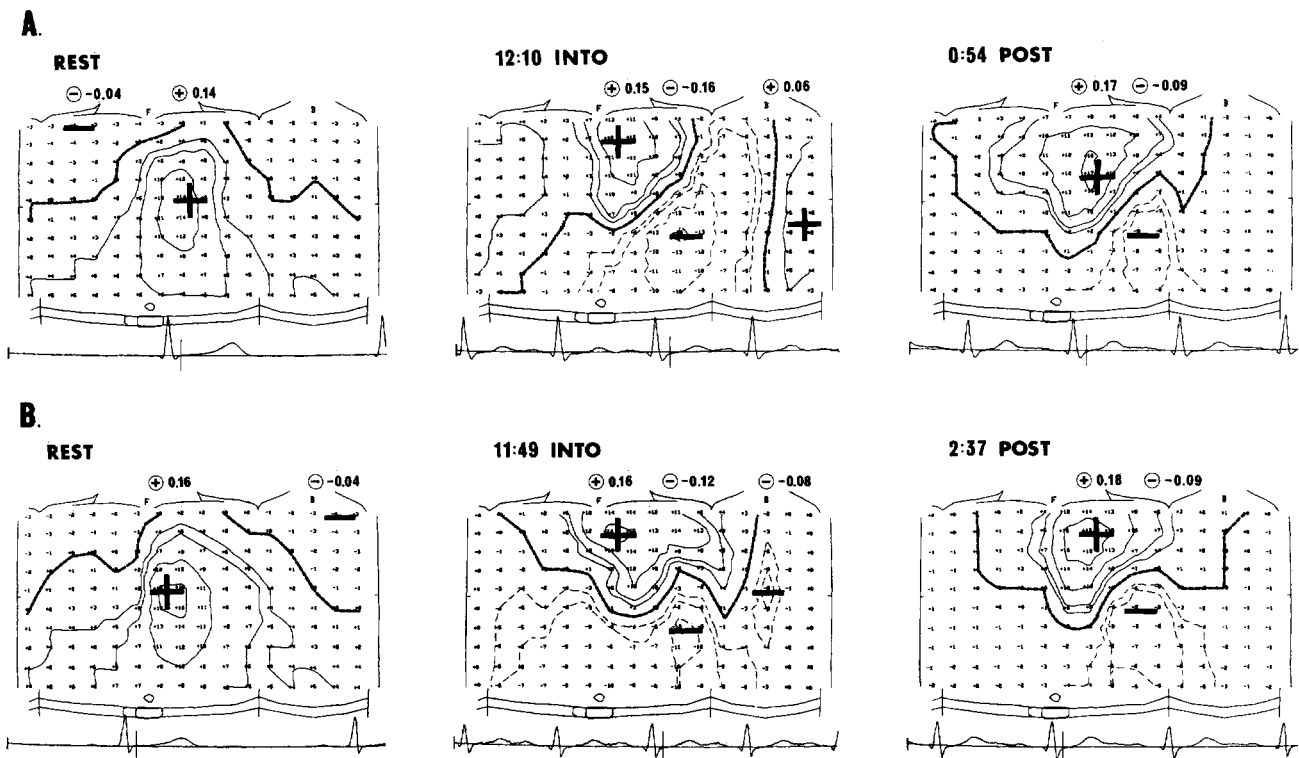


FIGURE 8. ST-segment maps at rest, during exercise and after exercise. Potential distributions during the ST segment are shown for two subjects. The time above the central map frame in each row indicates the time (in minutes and seconds) at which the ECG data were recorded relative to the beginning of the multistage exercise procedure. The time above the final map frame in each row indicates the time at which the ECG data were recorded relative to the cessation of exercise.

mV in the body surface maps from 12 of the 20 subjects (fig. 9). The magnitude decreased by more than 0.1 mV in the maps from three subjects and stayed nearly constant in the maps from the other five subjects. Immediately after exercise, the magnitudes of the T-wave potentials increased rapidly for all subjects, reaching a maximum value 30–90 seconds after cessation of exercise. In the resting maps the peak T-wave potentials ranged from 0.33–1.45 mV, while in the maps after exercise the peak T-wave potentials ranged from 0.59–2.69 mV. The percent increase in T-wave magnitude after exercise (with respect to the resting value) ranged from 30–260%.

For some subjects, the T-wave potential magnitudes returned to the resting values within 5 minutes after cessation of exercise, while for others they were still larger than the resting values when data collection was stopped 10 minutes after exercise.

Discussion

Changes in Body Surface Potential Distributions During Exercise

Although a decrease in the magnitude of the R wave in left precordial leads is often used to define a “normal” electrocardiographic response to exercise,²⁻⁸ the mechanisms underlying such R-wave changes are uncertain. A commonly proposed hypothesis relates the R-wave changes to the hemodynamic performance of

the heart as follows: During exercise, a reduction in end-diastolic volume occurs due to tachycardia, so the effective strengths of the radially oriented electrical sources are reduced due to the “Brody effect”.^{6-8, 16} This explanation seems unlikely, however, especially in light of recent radionuclide angiographic⁴¹ and echocardiographic⁴² studies suggesting that in most normal subjects end-diastolic volume stays the same or increases slightly during exercise. Also, R-wave magnitude is generally least immediately after exercise,⁵ while end-diastolic volume increases transiently after exercise.^{5, 42}

An increase in the distance between the exploring surface electrode and the heart due to increased inspiratory volume has also been suggested as a mechanism resulting in decreased R-wave magnitudes during exercise.⁵ In the present study, the potential maximum on the lower left anterior torso in mid-QRS (which was reflected in the peak amplitude of the R wave in lead V_6) was displaced downward on the map and reduced in magnitude during deep inspiration in exercise. However, at peak expiration during exercise, the potential maximum was often located at the same mapping point as in the maps at rest, and yet was still significantly smaller in magnitude than the corresponding maximum in the resting maps at either peak inspiration or expiration (during normal resting respiration). Thus, although respiratory variations were evident in the data, the changes in the magnitude

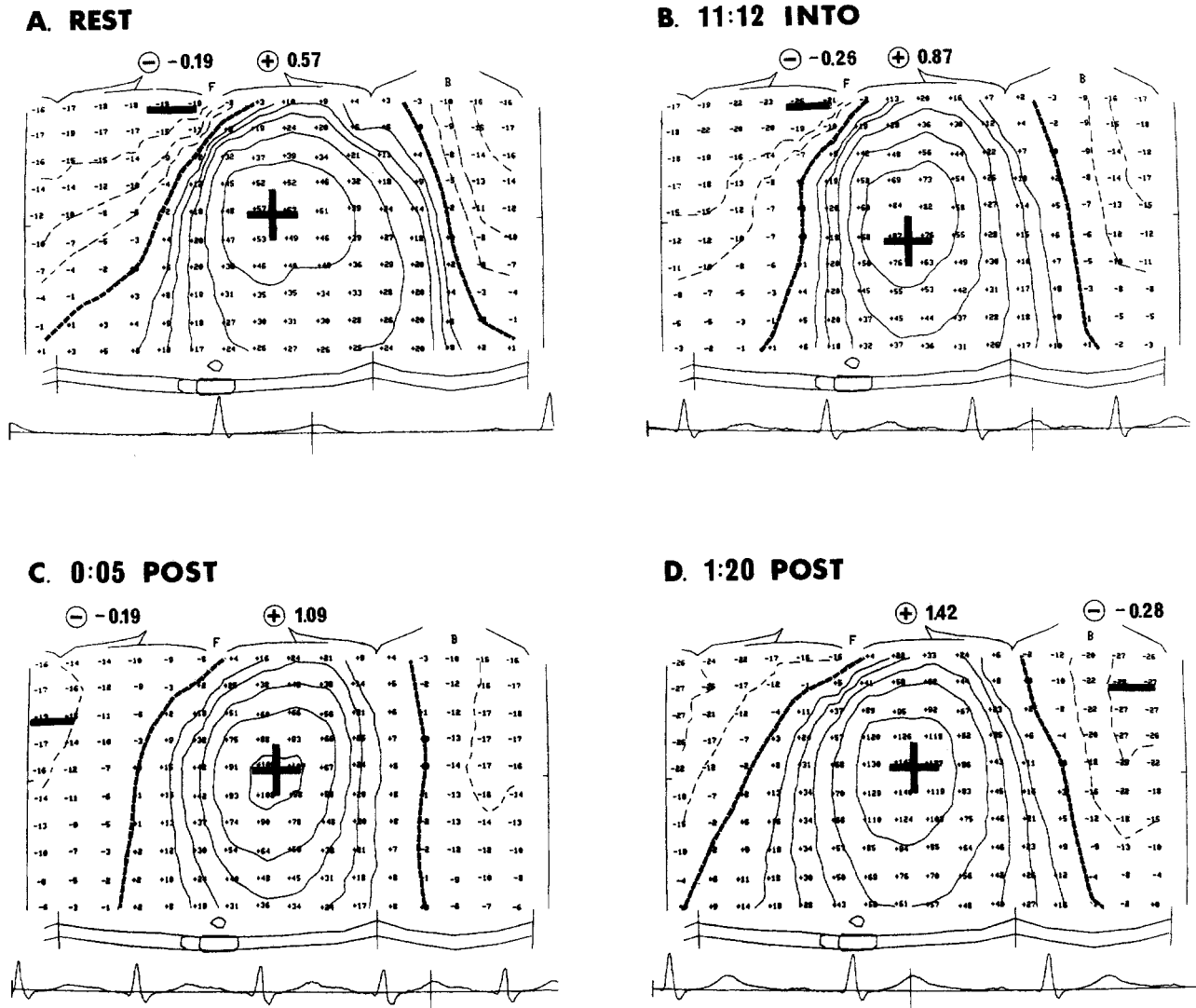


FIGURE 9. T-wave maps at rest, during exercise and after exercise. Body surface potential distributions are shown at the peak of the T wave for a single subject at rest (A), during exercise (B), at the end of exercise (C) and during recovery from exercise (D). The times at which the ECG data were recorded relative to the beginning (panel B) or the ending (panels C and D) of the multistage exercise procedure are indicated above each map frame.

of the left precordial maximum in mid-QRS during exercise appeared to be more than could be accounted for on the basis of increased respiration alone.

Reductions in the magnitude of the R wave in lead V_5 during exercise were accompanied in our data by changes in the body surface potential distributions in early QRS, changes in the shape of the early portion of the RMS map potential wave form and increases in QRS duration. This suggests that the changes in R-wave magnitude were related to changes in the sequence of activation of the ventricles during exercise. We offer the following qualitative description of the changes in early activation in the ventricles during exercise as a possible explanation of the observed changes in body surface potentials, based on a hypothesis that a delay (2–10 msec) occurred during exercise in the initial activation of the left ventricular free wall relative to the time of onset of excitation in the right ventricle and septum.

If a delay in the activation of the left ventricular free wall, relative to the onset of activation in the septum and right ventricle, were to occur during exercise, negative potentials would be expected in the left precordial region during early QRS (fig. 3) due to the dominant left to right spread of activation in the septum and right ventricle. As activation began in the left ventricle, the magnitude of the lower left minimum would decrease and the minimum would move toward the left side and back. If activation of the left ventricle were still at an early stage when right ventricular breakthrough occurred, generally lower potential magnitudes than in resting maps would be expected at the time of breakthrough and more complex potential patterns might result because the potentials on the body surface would be influenced relatively more by the diverging wave fronts around the depolarized region of the right ventricular epicardium.

With such an activation sequence, an initial rise in

RMS body surface potentials would be expected, as activation spread in the septum and right ventricle, followed by a drop in RMS potentials at breakthrough. The RMS potentials would then increase again rapidly as activation spread in the walls of the left ventricle. The time interval between the initial increase in the RMS wave form (corresponding to the beginning of ventricular activation) and the rapid rise preceding the peak RMS potential (corresponding to the spread of activation in the left ventricle) would be expected to be longer during exercise than at rest (fig. 7).

Generally, the body surface potential distributions during mid-QRS in normal subjects predominantly reflect the current from large activation wave fronts propagating from endocardium to epicardium in the wall of the left ventricle. As such, a change in the early activation sequence of the type suggested might be expected to have little effect on the basic pattern of potentials in mid-QRS as long as left ventricular activation proceeded in an endocardial-to-epicardial direction. Changes in the exact locations and shapes of the activation wave fronts during exercise, however, due to the change in early activation sequence might result in changes in the relative magnitudes of the maxima and minima and changes in the distributions of the lower-magnitude potentials distant from these major features, as were observed in this study. The decrease in the magnitude of the left precordial potential maximum in mid-QRS (and the R wave in lead V_6) during exercise might thus result from a change in the activation wave fronts in the wall of the left ventricle secondary to the changes in the initial activation sequence.

QRS duration increased during exercise in 11 of the 20 subjects. Previous studies of the exercise ECG^{2, 15} found no change in QRS duration. Variations in QRS duration of the magnitude found in this study (less than 10 msec) would probably be difficult to detect using ECG wave forms recorded during exercise from a small number of leads. Comparison of RMS map potential wave forms at rest and during exercise (fig. 7B), however, clearly indicate an increase in QRS duration. Although increases in QRS duration during exercise were found, they were consistently less than the delays during exercise in the rapid upstrokes of the RMS potential wave forms (fig. 7B). As a result, the RMS wave forms from some subjects showed a delay in the major upstroke during exercise but little change in overall duration (fig. 7C).

It has been suggested that J-point depression seen in left precordial leads recorded from normal subjects during exercise is at least in part a reflection of atrial repolarization (T_a) augmented at the J point during exercise by the shortening of the PR segment and by a possible increase in the magnitude of T_a .^{2, 36, 37} Changes in the early activation sequence of the ventricles during exercise suggest another mechanism for the changes in the body surface potential distribution during the ST segment. Potential distributions during early ventricular repolarization depend on both the distribution of cellular action potential shapes in the

myocardium and the sequence of ventricular activation.⁴³ Accordingly, if changes in the early activation sequence of the ventricles occur during exercise, changes in the potential distributions during the early ST segment might result from the changes in activation sequence alone, without any changes in action potential shapes during the plateau phase or any increase in the magnitudes of T_a potentials at the J point.

Mirvis et al.¹⁷ presented an analysis of precordial isopotential maps recorded from normal subjects using a grid of 42 electrodes on the left anterior precordium during multistage submaximal exercise procedures. Their results indicated significantly more precordial negativity during the ST segment in exercise than was found in our study, which they attributed to delayed activation near the base of the ventricles during the ST segment. We believe the different results were due to their choice of the TP junction as a potential reference. In our study, we used the end of the PR segment as a baseline reference because, in the absence of diastolic currents, it provides a better (but not perfect) estimate of "zero" potential at high heart rates.^{3, 29-31}

Figure 10 shows the body surface potentials during the ST segment recorded from a normal 23-year-old male early in the exercise procedure. The map shown in panel A is characterized by a prominent potential maximum in the left midsternal region, typical of normal ST-segment maps at rest,³⁴ but with a low-level potential minimum at the lower left of the maximum, typical of the results in this study at low work rates. The potential distribution in panel B is completely different, with a prominent potential minimum on the lower left anterior torso, a lower-level potential maximum near the upper sternum, and near zero potentials at the location of the potential maximum in panel A. The left precordial portion of the map in panel B is similar to the precordial maps presented by Mirvis et al.¹⁷ This potential distribution (panel B) contains large artifacts resulting from the non-zero potentials (from the merging of the U wave and P wave) at the time of the TP junction. The considerable difference between the isopotential maps in panels A and B emphasizes the need for careful selection of the potential references when processing ECG wave forms for body surface mapping during exercise.

Implications for the Study of the Exercise ECG

Exercise electrocardiographic testing has been in use for many years but the electrophysiologic mechanisms underlying the observed changes in ECG wave form shapes from both normal subjects and cardiac patients are only partially understood. The limitations of conventional lead systems used to study the exercise ECG are illustrated by the map pattern changes in the normal subjects of this study which strongly suggest changes in the early activation sequence of the ventricles during exercise. Electrophysiologic changes of this type are not apparent from visual examination of ECG wave forms alone because the resulting changes in wave form shape can-

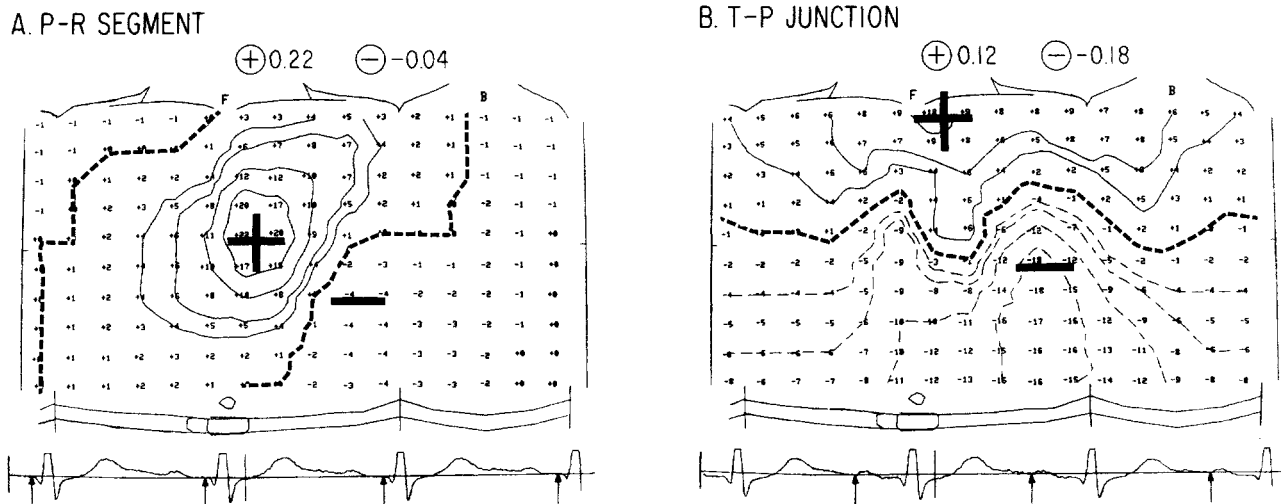


FIGURE 10. *Effects of voltage reference selection on ST-segment potential maps. (A) The potential distribution during the ST segment in exercise is referenced to the potentials just before QRS. The arrows on the time reference wave form indicate the voltage reference times. The vertical line through the ST segment of the second QRS-T complex indicates the time instant represented by the map. The vertical line to the left of the time reference trace indicates 1 mV of potential. (B) The potential distribution at the same instant of time during the ST segment is shown referenced to the potentials at the TP junction.*

not be distinguished from shape changes due to such factors as altered heart position or increased respiration.

Using total body surface isopotential maps, spatial distributions of the potentials over the surface of the torso can be examined at serial instants of time, as opposed to examining ECG wave form shapes from fixed electrode locations. Spatial shifts in the patterns of potentials in body surface maps, which can result in significant changes in ECG wave form shapes, are readily distinguished from pattern changes. In addition, significant changes in lower-magnitude potential distributions (near the beginning or ending of QRS for example), which may not result in clearly visible changes in wave form shape, can be examined using body surface maps. While precordial surface maps contain more spatial information about the ECG than measurements from a few scalar leads, many important features of body surface potential distributions are located outside of the limited region covered by precordial electrode arrays, and the lack of information about these features may adversely affect the interpretation of the ECG data.

Total body surface mapping during exercise has been difficult to perform because of technical problems in recording simultaneously from large electrode arrays during exercise. The development of limited lead mapping systems²²⁻²⁶ and portable systems for digitally recording multiple ECG channels⁴⁴ has made body surface mapping during exercise clinically practical. By using commercially produced stress test electrodes and cable systems, we could obtain high-quality body surface potential distributions during exercise without requiring wave form averaging or special modes of exercise to reduce recording artifact. Our results indicate both the technical feasibility of recording total body surface

maps during exercise and the importance of analyses of total body surface potential distributions for obtaining an improved physiologic understanding of ECG changes during exercise.

References

- Fortuin NJ, Weiss JL: Exercise stress testing. Reviews of contemporary laboratory methods. *Circulation* **56**: 699, 1977
- Bellet S, Eliakim M, Deliyannis S, Figallo EM: Radioelectrocardiographic changes during strenuous exercise in normal subjects. *Circulation* **25**: 686, 1962
- Bruce RA, Mazarella JA, Jordan JW, Green E: Quantitation of QRS and ST segment responses to exercise. *Am Heart J* **71**: 455, 1966
- Kentala E, Heikkilä J, Pyörölä K: Variation of QRS amplitude in exercise ECG as an index predicting results of physical training in patients with coronary heart disease. *Acta Med Scand* **194**: 81, 1973
- Kentala E, Luurila O: Response of R wave amplitude to postural changes and to exercise. A study on healthy subjects and patients surviving myocardial infarction. *Ann Clin Res* **7**: 258, 1975
- Bonoris PE, Greenberg PS, Christison GW, Castellanet MJ, Ellestad MN: Evaluation of R wave amplitude changes versus ST segment depression in stress testing. *Circulation* **57**: 904, 1978
- Bonoris PE, Greenberg PS, Castellanet MJ, Ellestad MN: Significance of R wave amplitude during treadmill stress testing: angiographic correlation. *Am J Cardiol* **41**: 846, 1978
- Christison GW, Bonoris PE, Greenberg PS, Castellanet MJ, Ellestad MN: Predicting coronary artery disease with treadmill stress testing: changes in R wave amplitude compared with ST segment depression. *J Electrocardiol* **12**: 179, 1979
- Mason RE, Likar I: A new system for multiple lead exercise electrocardiography. *Am Heart J* **71**: 196, 1966
- Mason RE, Likar I, Biern RO, Ross RS: Multiple lead exercise electrocardiography. *Circulation* **36**: 517, 1967
- Chaitman BR, Waters DD, Bourassa MG, Tubau JF, Wagniar P, Ferguson RJ: The importance of clinical subsets in interpreting maximal treadmill exercise test results: the role of multiple-lead ECG systems. *Circulation* **49**: 560, 1979

12. Blomqvist GC: The Frank lead exercise electrocardiogram: quantitative study based on averaging techniques and digital computer analysis. *Acta Med Scand* **178** (suppl 440), 1965
13. Hornsten JR, Bruce RA: Computed ST forces of Frank and bipolar electrocardiograms. *Am Heart J* **78**: 346, 1969
14. Dower GE, Bruce RA, Pool J, Simoons ML, Niederberger MW, Meilink LJ: Ischemic polarcardiographic changes induced by exercise. *Circulation* **48**: 725, 1973
15. Simoons ML, Hugenholtz PG: Gradual changes in ECG waveform during and after exercise in normal subjects. *Circulation* **52**: 570, 1975
16. Simoons ML, Hugenholtz PG: Estimation of the probability of exercise induced ischemia by quantitative ECG analysis. *Circulation* **56**: 552, 1977
17. Mirvis DM, Keller FW, Cox JW, Zettergren DG, Dowdie RF, Ideker RD: Left precordial isopotential mapping during supine exercise. *Circulation* **56**: 245, 1977
18. Fox KM, Selwyn AP, Shillingford JP: A method for praecordial surface mapping of the exercise electrocardiogram. *Br Heart J* **40**: 1339, 1978
19. Fox KM, Selwyn AP, Shillingford JP: Precordial electrocardiographic mapping after exercise in the diagnosis of coronary artery disease. *Am J Cardiol* **43**: 541, 1979
20. Schubert E, Eckoldt K, Kästner R: The electric field of the cardiac repolarization in physical work. *Adv Cardiol* **16**: 32, 1976
21. Block P, Lenaers A, Tiberghien J, Coussaert E, van Thiel E, Lebedelle M, Raadschelders I, Bourgain R, Kornreich F: Surface maps and myocardial scanning at rest and during exercise: comparison with coronary angiography. *Acta Cardiologica* **31**: 467, 1976
22. Barr RC, Spach MS, Herman-Giddens GS: Selection of the number and positions of measuring locations for electrocardiography. *IEEE Trans Biomed Eng BME-18*: 125, 1971
23. Warren RB: Determining the number and positions of measuring locations for body surface potential mapping. Ph.D. dissertation, Duke University, 1977
24. Lux RL, Smith CR, Wyatt RF, Abildskov JA: Limited lead selection for estimation of body surface potential maps in electrocardiography. *IEEE Trans Biomed Eng BME-25*: 270, 1978
25. Lux RL, Burgess MJ, Wyatt RF, Evans AK, Vincent GM, Abildskov JA: Clinically practical lead systems for improved electrocardiography: comparison with precordial grids and conventional lead systems. *Circulation* **59**: 356, 1979
26. Warren RB, Barr RC, Spach MS: Determining the minimum number and best placement of leads for a practical clinical body surface mapping system. (abstr) *Circulation* **56** (suppl III): III-200, 1977
27. Miller WT, Spach MS, Barr RC, Warren RB, Herman-Giddens GS: Isopotential surface maps from normal adults during exercise. (abstr) *Circulation* **58** (suppl II): II-65, 1978
28. Barr RC, Herman-Giddens GS, Spach MS, Warren RB, Gallie TM: The design of a real-time computer system for examining the electrical activity of the heart. *Comput Biomed Res* **9**: 445, 1976
29. Spach MS, Barr RC, Warren RB, Benson DW, Walston A, Edwards SB: Isopotential body surface mapping in subjects of all ages: emphasis on low-level potentials with analysis of the method. *Circulation* **59**: 805, 1979
30. Master AM, Friedman R, Dack S: The electrocardiogram after standard exercise as a functional test of the heart. *Am Heart J* **24**: 777, 1942
31. Lloyd-Thomas HG: The effect of exercise on the electrocardiogram in healthy subjects. *Br Heart J* **23**: 260, 1961
32. Meyer CR, Keiser HN: Electrocardiogram baseline noise estimation and removal using cubic splines and state-space computation techniques. *Comput Biomed Res* **10**: 459, 1977
33. Taccardi B: Distribution of heart potentials on the thoracic surface of normal human subjects. *Circ Res* **12**: 341, 1963
34. Spach MS, Barr RC, Benson DW, Walston A, Warren RB, Edwards SB: Body surface low-level potentials during ventricular repolarization with analysis of the ST segment. Variability in normal subjects. *Circulation* **59**: 822, 1979
35. Taccardi B: Body surface distribution of equipotential lines during atrial depolarization and ventricular repolarization. *Circ Res* **19**: 865, 1966
36. Lepeschkin E: Exercise tests in the diagnosis of coronary heart disease. *Circulation* **22**: 986, 1960
37. Lepeschkin E: Physiological factors influencing the electrocardiographic response to exercise. *In* Measurements in Exercise Electrocardiography. The Ernst Simonson Conference, edited by Blackburn H. Springfield, Illinois, Charles C Thomas, 1969, pp 363-385
38. Yu PNG, Bruce RA, Lovejoy FW, McDowell ME: Variations in electrocardiographic responses during exercise. Studies of normal subjects under unusual stresses and of patients with cardiopulmonary diseases. *Circulation* **3**: 368, 1951
39. Lepeschkin E, Surawicz B: Characteristics of true positive and false-positive results of electrocardiographic master two-step exercise tests. *N Engl J Med* **258**: 511, 1958
40. Simonson E: Use of electrocardiogram in exercise tests. *Am Heart J* **71**: 196, 1966
41. Rerych SK, Scholz PM, Newman GE, Sabiston DC, Jones RH: Cardiac function at rest and during exercise in normals and in patients with coronary heart disease: evaluation by radionuclide angiography. *Ann Surg* **197**: 449, 1978
42. Stein RA, Michelli D, Fox EL, Krasnow N: Continuous ventricular dimensions in man during supine exercise and recovery. An echocardiographic study. *Am J Cardiol* **41**: 655, 1978
43. Spach MS, Barr RC: Origin of epicardial ST-T wave potentials in the intact dog. *Circ Res* **39**: 475, 1976
44. Herman-Giddens GS, Warren RB, Shifflette JJ, Miller WT, Spach MS, Barr RC: A portable system for acquiring body surface potentials. (abstr) Proc 32nd ACEMB, Denver, 1979, p 187